



HAL
open science

A comparative study of alanine adsorption and condensation to peptides in two clay minerals

Fabírcia de Castro Silva, Luciano Clécio Brandão Lima, Edson Silva-Filho, Maria Gardennia Fonseca, Jean-François Lambert, Maguy Jaber

► To cite this version:

Fabírcia de Castro Silva, Luciano Clécio Brandão Lima, Edson Silva-Filho, Maria Gardennia Fonseca, Jean-François Lambert, et al.. A comparative study of alanine adsorption and condensation to peptides in two clay minerals. *Applied Clay Science*, 2020, 192, pp.105617. 10.1016/j.clay.2020.105617 . hal-02887409

HAL Id: hal-02887409

<https://hal.sorbonne-universite.fr/hal-02887409v1>

Submitted on 2 Jul 2020

HAL is a multi-disciplinary open access archive for the deposit and dissemination of scientific research documents, whether they are published or not. The documents may come from teaching and research institutions in France or abroad, or from public or private research centers.

L'archive ouverte pluridisciplinaire **HAL**, est destinée au dépôt et à la diffusion de documents scientifiques de niveau recherche, publiés ou non, émanant des établissements d'enseignement et de recherche français ou étrangers, des laboratoires publics ou privés.

1 **A comparative study of alanine adsorption and condensation to peptides in two**
2 **clay minerals**

3 **Fabrcia de Castro Silva^{1,2,3}, Luciano Clcio Brandao Lima^{1,2}, Edson C. Silva-**
4 **Filho², Maria Gardennia Fonseca⁴, Jean-Francois Lambert⁵, Maguy Jaber*¹**

5 maguy.jaber@sorbonne-universite.fr

6 ¹ **LAMS**, Sorbonne Universit, CNRS UMR8220, 75005 Paris, France

7 ² **LIMAV**, Univ. Federal do Piau, UFPI, 64049-550 Piau, Brazil

8 ³ **CSHNB**, Uni. Federal do Piau, UFPI, 64607-670, Piau, Brazil

9 ⁴ **NPE-LACOM**, Univ. Federal da Paraiba – UFPB, Joao Pessoa, 58051-900 Paraiba,
10 Brazil

11 ⁵ **LRS**, Sorbonne Universit, UMR 7149, 75005 Paris, France

12
13 **ABSTRACT**

14 The polycondensation of amino acids to oligopeptides is an important step in the
15 origins of life, and known to be effective on several mineral surfaces. The data available
16 on clay mineral surfaces are heterogeneous and sometimes contradictory, however. The
17 objective of the present work is to investigate the adsorption of a selected amino acid,
18 alanine, in expanding and non-expanding clays and then study the possible peptide
19 condensation by thermal activation. A multi-technique approach was used, including
20 macroscopic measurements of the adsorption process (adsorption isotherms and pH-
21 metry), and in situ molecular-level characterization of the solids obtained (X-ray
22 diffraction, thermogravimetric analysis and infrared spectroscopy). The results indicate
23 that only weak interaction is established between alanine molecule and kaolinite
24 surfaces, most of the deposited molecules being only physically retained. Thermal
25 activation of alanine/kaolinite only led to desorption. In contrast, higher-energy
26 adsorption mechanisms were at play in hectorite, including cation exchange and
27 coordinative adsorption to the interlayer ions, and alanine species adsorbed in this way
28 were observed to form cyclic dimers upon activation between 160 and 270 °C.

29 **Keywords:** Kaolinite, hectorite, alanine, Prebiotic Chemistry, peptide bond.

30 1 INTRODUCTION

31 How did life emerge? This question keeps intriguing researchers in different fields as
32 well as non-scientists. One of its aspects is prebiotic chemistry, the study of the
33 primordial formation of biomolecules before the appearance of micro-organisms, and
34 research scientists start to realize that prebiotic pathways may have originated on the
35 surface of ancient minerals (Fontecilla Camps, 2019). Bernal (Bernal, 1949) was the
36 first researcher to associate clay minerals with the origin of life. According to his
37 hypothesis, clays could have played an important role in amino acid concentration,
38 which was necessary to induce their polymerization to peptides, as they are good
39 adsorbents (Ramos and Huertas, 2013; Villafane-Barajas et al., 2018; Zaia, 2012).

40 Now, clays have been invoked in several other roles connected with Origins of Life
41 studies, including confinement - allowing to concentrate, confine and protect molecules,
42 creating a “safe” environment for proto-biochemical reactions (Yang et al., 2013). Here,
43 however, we will concentrate on their potential effect on amino acids adsorption and
44 polymerization. Bernal’s hypothesis has gained strength over the years. First, clay
45 minerals are widely distributed, have been historically prevalent along the whole
46 timeline of geological and biological events on Earth, and have affinity for organic
47 molecules (Aguilar-Ovando and Negrón-Mendoza, 2015; Carneiro et al., 2011;
48 Georgelin et al., 2015; Kalra et al., 2000; Pedreira-Segade et al., 2016; Ponnampereuma
49 et al., 1982). Second, amino acids polymerization has been observed experimentally in
50 the presence of clay minerals starting in the 1970’s, (Bujdák et al., 1994; Jaber et al.,
51 2014; Lahav et al., 1978; Paecht-Horowitz et al., 1970). A summary of work related to
52 amino acids surface polymerization on various supports may be found in (Lambert,
53 2008). The implications of the formation of oligopeptides to “kick-start” the evolution
54 of Life are discussed e.g. in Brack, 2008.

55 However, these studies mostly have an exploratory character. Little justification is
56 offered for the choice of the mineral phases to assess peptide formation reactivity; the
57 experimental procedures applied may be quite different, and the experimental results
58 have little in common beyond the bare occurrence of peptide formation (see Tables 1
59 and 2). Clays are not systematically compared with other minerals, much less between
60 themselves. Two important exceptions may be found in the work of Bujdák and Rode
61 ((Bujdák and Rode, 1999b) and (Bujdák and Rode, 1999a), respectively). Recent work
62 on amino acids polymerization more often uses silica or titania as a support, in part for
63 reasons regarding the ease of characterization (Guo and Holland, 2015; Martra et al.,
64 2014; Sakhno et al., 2019) or, if clays are used, montmorillonite is often chosen as a
65 generic smectite (Kollár et al., 2003; Bu et al., 2019). In the present paper, we report on
66 the comparative polymerization ability of two different clay minerals, kaolinite and
67 hectorite, that differ in layer structure as well as in layer charge.

68 Kaolinite $[\text{Al}_2\text{Si}_2\text{O}_5(\text{OH})_4]$ belongs to the kaolin subgroup of minerals, and is one of the
69 most common of the aluminosilicate clay minerals. Kaolinite has a 1:1 layer structure
70 (T-O), exhibits two distinctly different types of surface, base planes (001) and edge
71 planes (110) and (010). The basal planes are anisotropic: one face exposes tetrahedral
72 siloxane surface ($-\text{Si}-\text{O}-\text{Si}-$), and the opposite one consists of an octahedral gibbsite-
73 like $(\text{Al}(\text{OH})_3)$ sheet. The basal planes are electrically neutral, but the reactivity of
74 kaolinite surfaces is often driven by hydroxyl groups located at the edge planes, whose
75 net charge is pH depend (Spence and Kelleher, 2012). Studies reporting adsorption of
76 organic molecules in kaolinites have appeared extensively in the literature (Duarte-Silva
77 et al., 2014).

78 Smectites make up another important group of clay minerals that likely occurred widely
79 in the environments from weathering of volcanic rocks on the early Earth. They are

80 characterized by a 2:1 layer structure (T-O-T), which consists of an octahedral sheet
81 sandwiched between two tetrahedral sheets (BU et al., 2019b). Due to the negative layer
82 charge originating from substitutions, they generally exhibit cation exchange capacities
83 in the range of 50 to 100 meq.g⁻¹. Hectorite is a well-known representative mineral of
84 the smectite family. The ideal chemical formula of hectorite is
85 Na_{0.3}Mg_{2.7}Li_{0.3}Si₄O₁₀(OH)₂, in which the layer structure is composed of an Mg and Li-
86 containing octahedral sheet sandwiched between two tetrahedral Si-containing sheets. It
87 is a trioctahedral smectite, and the origin of the layer charge is in the octahedral sheet,
88 so that the negative layer charge is more spread out (less localized) than in other
89 smectites such as saponites where the electric charge originates from tetrahedral sheet.

90 The objective of the present work is to characterize the interaction between a simple
91 amino acid, alanine (Ala) and these two clay minerals, by means of the different
92 characterizations (X-Ray Diffraction, Thermogravimetric Analysis and Infrared
93 spectrometry), and especially to check whether or not these clays give rise to peptide
94 formation. As can be seen in table 1, studies of amino acid (AA) polymerization on
95 kaolinite supports are rather heterogeneous and the systems were activated in very
96 different conditions, with correspondingly different results. Studies on hectorite have
97 been carried out in more homogeneous conditions, mostly involving wetting-and-drying
98 cycles, with a body of data obtained by Bujdák, Rode and coworkers. It is generally
99 found to induce significant polymerization of at least small amino acids (such as Ala
100 and Gly), although some contradictions are found, e.g. as regards its relative efficiency
101 as compared to montmorillonite. The activation conditions applied, however, involve
102 quite low drying temperatures that only lead to low or moderate peptide yields.

103 In the present study, we chose a simple activation by heating in dry air at the target
104 temperature because wetting-and-drying procedures involve many steps of hydrolysis,

105 condensation and bond rearrangement and the underlying chemistry is difficult to
 106 understand.

107 Table 1: Studies that reported amino acids polymerization on kaolin or kaolinite clays.

108 AA = amino acid, Gly = glycine, Ala = Alanine, Val = valine, Asp = aspartic acid, Ser =
 109 serine, Phe = phenylalanine; Gly₂ = linear Glycylglycine, DKP = diketopiperazine
 110 (cyclic dimer). TF = temperature fluctuation, WD = wetting and drying.

Ref	Amino acid(s) adsorbed	Activation procedure	Activation temperatures	Results
(Jackson, 1971)	Asp, Ser, Phe	Heating in sealed tubes in presence of solution	80 °C, up to 10 days	Unspecified peptides, up to 25%. Enantioselectivity claimed
(Lahav et al., 1978)	Gly	TF cycles, compared with WDTF cycles	dehydration 60 °C, then heating at 94 °C	Up to Gly ₅ . WDTF much more efficient than TF
(White et al., 1984)	Gly	Probably heating in vacuo	70 to 145 °C	Low amounts of unspecified polymers
(Ito et al., 1990)	Gly, Ala, Val, Asp together – introduced as the amides!	7 WD cycles with constant adding of AA	Drying at 100 °C, open beaker	Very long linear polymers
(Zamaraev et al., 1997)	Gly	Hydrothermal reactions (no drying)	100 to 150 °C, autogenic pressure	Slow formation of Gly ₂ .
(Bujdák and Rode, 1999a)	Gly, Gly ₂ , Gly+Ala, Gly ₂ +Ala	5 WDTF cycles	Drying at 80 °C	Small amounts (≤2%) of Gly and DKP. Ala less reactive than Gly
(Meng et al., 2007)	Gly	Direct heating in air gas flow	In steps, followed by in situ IR, from 110 to 510 °C	Amide bands, assigned to DKP, present from 210 to 310 °C
(Dalai et al., 2017)	Gly	Dry heating under N ₂	200 or 250 °C	Mostly desorbs, 5% transformed to Gly ₂ and DKP

111

112 Table 2: Studies that reported amino acids polymerization on hectorite clays. Mt,
 113 montmorillonite; Hec, hectorite; Kao, kaolinite. Val = valine, Pro = proline, Lys =
 114 lysine, Tyr = tyrosine. SIPF = salt-induced peptide formation.

Ref	Amino acid(s) adsorbed	Activation procedure	Activation temperatures	Results
(Paecht-Horowitz, 1978)	Ala, Lys – introduced as the adenylates!	?	?	Gives longer polymers than Mt
(Bujdák and Rode, 1997; Jackson, 1971)	Ala, Gly+Ala, Gly ₂ +Ala, DKP	1 to 14 WDTF cycles, with variable amounts of water.	Drying at 80 °C	Better yields than Mt - More efficient for chain elongation than for initial peptide formation.
(Le Son et al., 1998)	Gly, Ala	WDTF cycles, with constant adding of AA; also carried out in the presence of CuCl ₂ and NaCl (SIPF)	Drying at 80 °C	Hec less efficient than Mt.
(Porter et al., 1998)	Gly	10 WDTF cycles	Drying at 90 °C	Large yields of DKP and Gly ₂ , smaller yields of peptides up to Gly ₆
(Bujdák and Rode, 1999a) (cf. Table 1, line 6)	Gly, Gly ₂ , Gly+Ala, Gly ₂ +Ala	5 WDTF cycles	Drying at 80 °C	Hec gives polymer yields up to 10 times higher than Kao
(Bujdák and Rode, 1999b)	Gly, Ala, Pro, Val, Leu, and mixtures	7 WDTF cycles	Drying at 85 °C	Gly gives linear and cyclic dimers, Ala less reactive; other AAs unreactive.
(Porter et al., 2001)	Gly, Tyr	10 WDTF cycles	Drying at 85 °C	Cu ²⁺ -hectorite was tested – somewhat less efficient than Mt

115

116 2 EXPERIMENTAL PART

117 2.1. Chemicals

118 Kaolinite purchased from sigma Aldrich (CAS Number: 1318-74-7) with the following
119 theoretical formula per half unit cell $\text{Al}_2(\text{Si}_2\text{O}_5)(\text{OH})_4$, deionized water, sodium acetate
120 (sigma aldrich, 99% wt), magnesium acetate tetrahydrate (sigma Aldrich, 99% wt),
121 lithium acetate (sigma aldrich, 99.5% wt), sodium silicate solution (sigma aldrich, CAS
122 Number: 127-09-3), L-alanine (sigma Aldrich, 98% wt), hydrochloric acid (sigma
123 aldrich, 37% wt), sodium hydroxide (sigma aldrich, 99% wt), acetic acid (sigma
124 Aldrich, 99% wt) ammonia (sigma Aldrich, 28% wt). All chemicals applied in this work
125 were purchased from Aldrich or Sigma-Aldrich with an analytical grade and used
126 without any previous purification.

127 2.2 Synthesis of the hectorite (HecS)

128 For the synthesis of sodium hectorite, a first solution of sodium acetate (0.4 g) in water
129 15g) and sodium silicate (14.8 g) was prepared. A second solution of deionized water
130 (35g), lithium acetate (0.2g), magnesium acetate (9.1g), and acetic acid was added to the
131 first one under stirring. The composition corresponded to the following theoretical
132 formula: $\text{Na}_{0.3}[(\text{Si}_4)(\text{Mg}_{2.7}\text{Li}_{0.3})]\text{O}_{10}(\text{OH})_2$ (formula of Hectorite per half unit cell for a
133 substitution ratio of Magnesium by lithium cations of 0.3) The hydrogels were aged
134 under stirring at room temperature for 6 h and then were autoclaved for reaction at 300
135 °C and 90 bar for 6 h. The autoclave was cooled to room temperature and the solid
136 product was washed thoroughly with distilled water and separated by centrifugation.
137 The solids were then dried at 50 °C for 24 h.

138 2.3 Samples prepared by experimental isotherms

139 Alanine solutions were used in the 0.05-1.25 mol.L⁻¹ concentration range (Table 3).
140 Thus, 150.0 mg of the adsorbent material were contacted with the amino acid solution
141 (5.0 ml for Kao and 15.0 ml for HecS) and subjected to mechanical stirring for 2 h.
142 They were then centrifuged and analyzed.

143 Table 3: Specific alanine concentrations used for deposition on kaolinite and hectorite.

Concentration	Sample #
0.05 mol.L ⁻¹	1
0.10 mol.L ⁻¹	2
0.15 mol.L ⁻¹	3
0.20 mol.L ⁻¹	4
0.35 mol.L ⁻¹	5
0.50 mol.L ⁻¹	6
0.65 mol.L ⁻¹	7
0.85 mol.L ⁻¹	8
1.0 mol.L ⁻¹	9
1.25 mol.L ⁻¹	10

144

145 The experimental adsorption isotherm was made in duplicate.

146 **2.5 Heat treatment of the samples**

147 Samples obtained by adsorption were subjected to heat treatment (20.0 mg) in a
148 temperature-programmed oven in a U-shaped cell, with a heating ramp of 5 °C.min⁻¹
149 and different final temperatures: 280 °C for Kao and Ala/Kao 5 (0.35 mol.L⁻¹) samples,

150 160 °C and 270 °C for Ala/HecS 1 (0.05 mol.L⁻¹), Ala/HecS 2 (0.1 mol.L⁻¹) and
151 Ala/Kao 5 (0.35 mol.L⁻¹), under a dry oxygen flow with a flow rate of 100 mL.min⁻¹.

152

153 **2.6 Characterization**

154 **2.6.1 Fourier transform infrared (FT-IR)**

155 FT-IR spectra were recorded in the transmission mode in KBr pellets (7.5 mg of the
156 substances in 142.5 mg KBr), using a Magna-IR 500 series II spectrometer, with 128
157 scans, between 4000 and 400 cm⁻¹. Data were analyzed with the software OMNIC S.P.
158 52.

159 **2.6.2 X-ray diffraction (XRD)**

160 Powder X-ray diffractograms were recorded using a D8 Advance Bruker-AXS Powder
161 X-ray diffractometer and working with the Cu K α radiation ($\lambda = 1.5404 \text{ \AA}$). The
162 diffractograms were recorded between 5-70° (2 θ), with a scan rate of 0.5 °.min⁻¹.

163 **2.6.3 Thermal analysis (TG/DTG)**

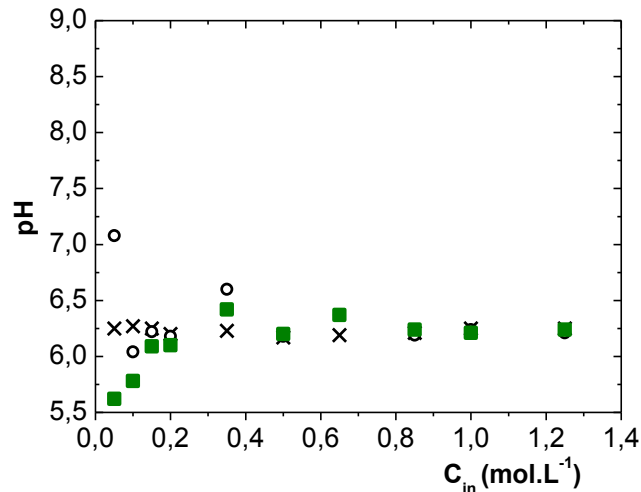
164 Thermogravimetric analyses were carried out using a TA Instrument SDT Q600
165 analyzer. The heating rate was 5 °C.min⁻¹ from 25 °C to 1000 °C, under a dry air flow of
166 10 mL.min⁻¹, and using alumina pans.

167 **3. RESULTS**

168 **3.1 Alanine on kaolinite**

169 The adsorption process was followed by measuring the pH of the alanine solutions
170 before contact, immediately after contact, and after 2 hours **equilibrium** prior to

171 separation of the solids. As shown in Figure 1, the pH does not evolve much, except in
172 the most dilute solutions where a small acidic drift is observed. At higher
173 concentrations, it has the constant value of 6.2, dictated by the alanine buffer.

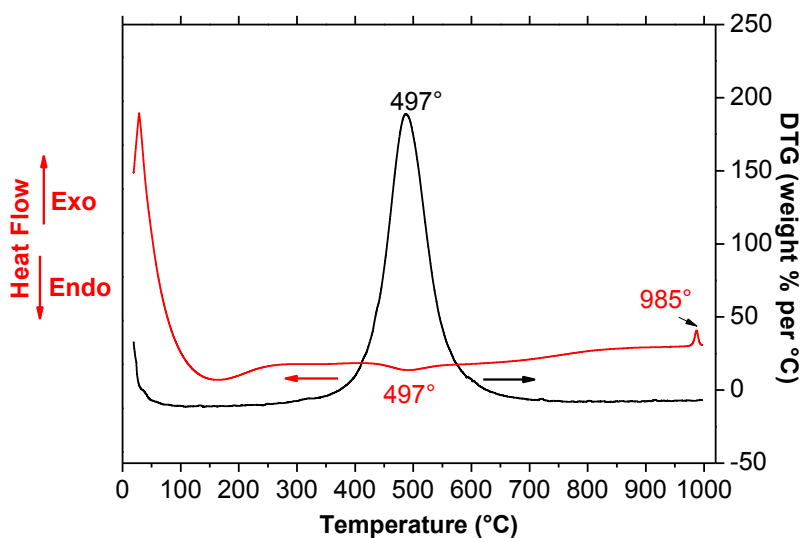


174

175 *Figure 1: pH evolution upon contact of Ala solutions with kaolinite, as a function of the*
176 *initial [Ala] concentration. Crosses, before contact; empty circles, immediately after*
177 *contact; full squares, after equilibrium.*

178

179 In TG, raw kaolinite (Figure 2) does not lose any significant weight prior to 300 °C. In
180 particular, it does not hold physisorbed water. At higher temperatures, it presents a
181 single, slightly endothermic weight loss, peaking at 497 °C in our conditions, and
182 corresponding to the transformation to metakaolin (Lambert et al., 1989), with a 14.5 to
183 14.9% weight loss. Finally, at 985 °C, the transformation to mullite is betrayed by a
184 sharp exothermic DTA signal without weight loss.

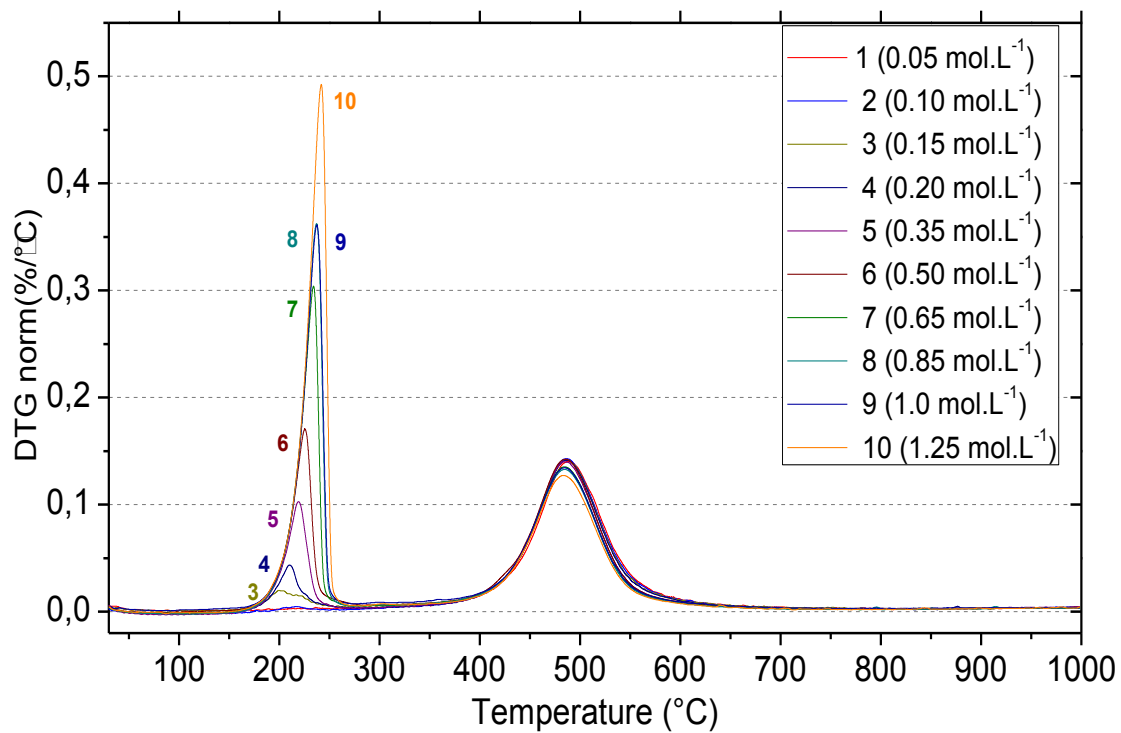


185

186

Figure 2: Thermal analysis of raw kaolinite.

187 The kaolinite to metakaolinite transition event is unchanged in Ala/Kao samples. The
 188 latter, however, also present an additional, endothermic weight loss in the 175-265 °C
 189 region, whose intensity increases monotonously with the amount of alanine that was
 190 contacted to the kaolinite (Figure 3). The lack of any IR bands except those of the
 191 kaolinite support (vide infra) after this thermal event indicates that all the organic matter
 192 is lost before 265 °C, and thus the weight loss of the endothermic event can be used to
 193 determine the amount of alanine (or alanine-derived compounds) contained in the initial
 194 dry solid.



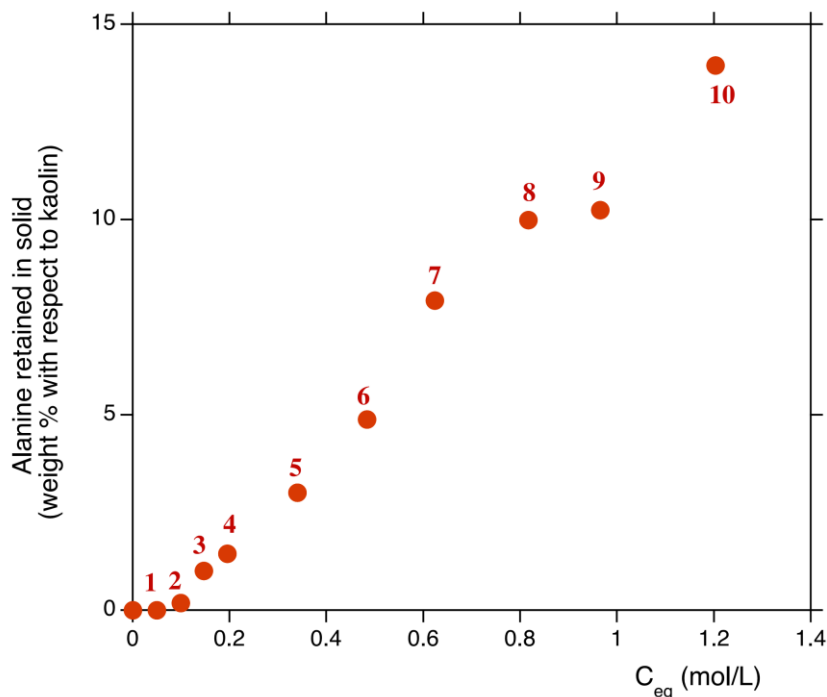
195

196 *Figure 3: DTG traces of raw kaolinite, and Ala/Kao samples containing increasing*
 197 *amounts of alanine (1 to 10).*

198

199 The amount of alanine retained is plotted as a function of the solution concentration in
 200 Figure 4.

201



202

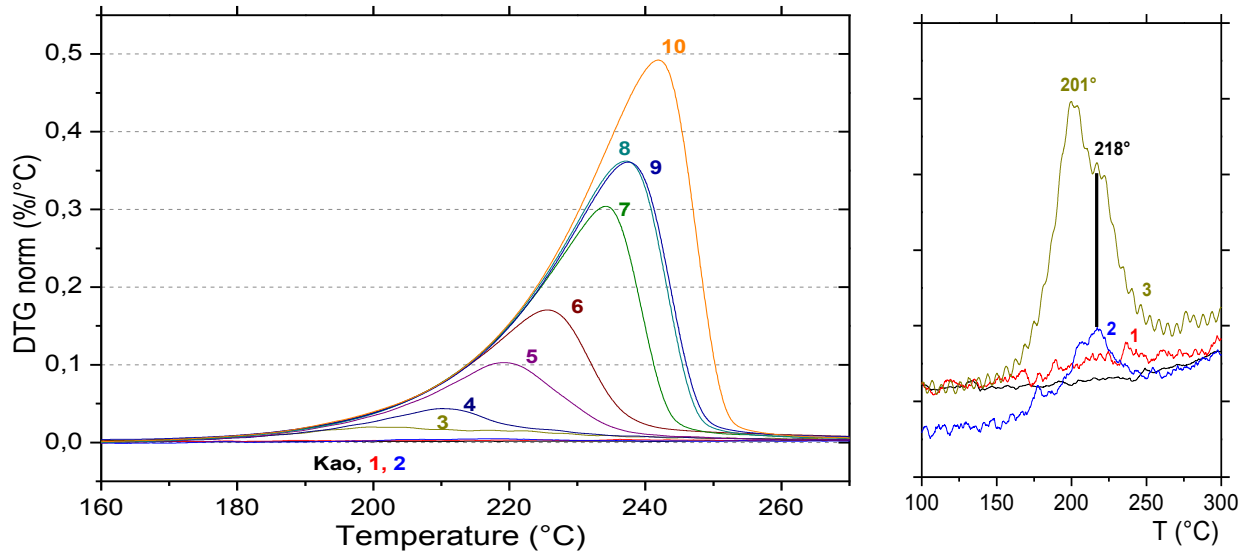
203 *Figure 4: Amounts of alanine (from TG quantification) retained in solid Ala/Kao*
 204 *samples as a function of the final concentration in solution (increasing concentrations*
 205 *from 1 to 10)*

206 In principle, it could be interpreted as an adsorption isotherm. In this case however, and
 207 since no washing step was applied, it is likely that a small amount of the alanine-
 208 containing solution was physically retained by the solid prior to drying – the amount
 209 retained is indeed almost linearly proportional to the initial solution concentration,
 210 corresponding to about 4% of the total amount of alanine in solution; in other words,
 211 kaolinite would physically retain about 1.3 mL solution per gram. The only other
 212 published “adsorption isotherm” for an amino acid (Gly) on kaolinite has the same
 213 general aspect (Meng et al., 2007).

214 The elimination of all the organic matter in a single, endothermic event suggests a
 215 simple desorption is happening. Bulk alanine sublimates under the same heating
 216 conditions, with a maximum weight loss rate at 289 °C (T_{max}). A close-up of the alanine

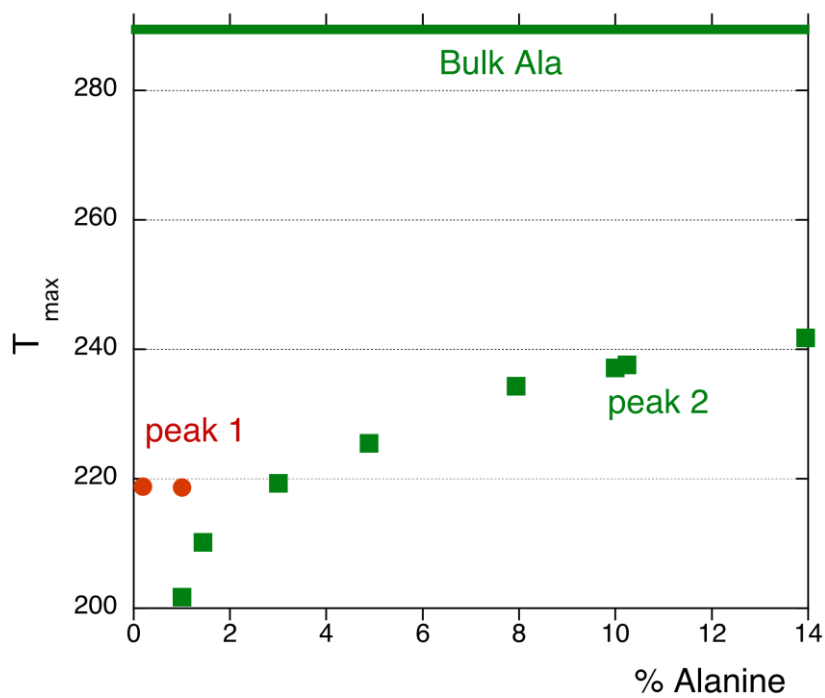
217 elimination event in our samples indicates that the T_{max} increases with the amount of
218 alanine in our samples (Figures 5 and 6).

219



220 *Figure 5: same as Figure 3, close-up of the alanine elimination region*

221



222

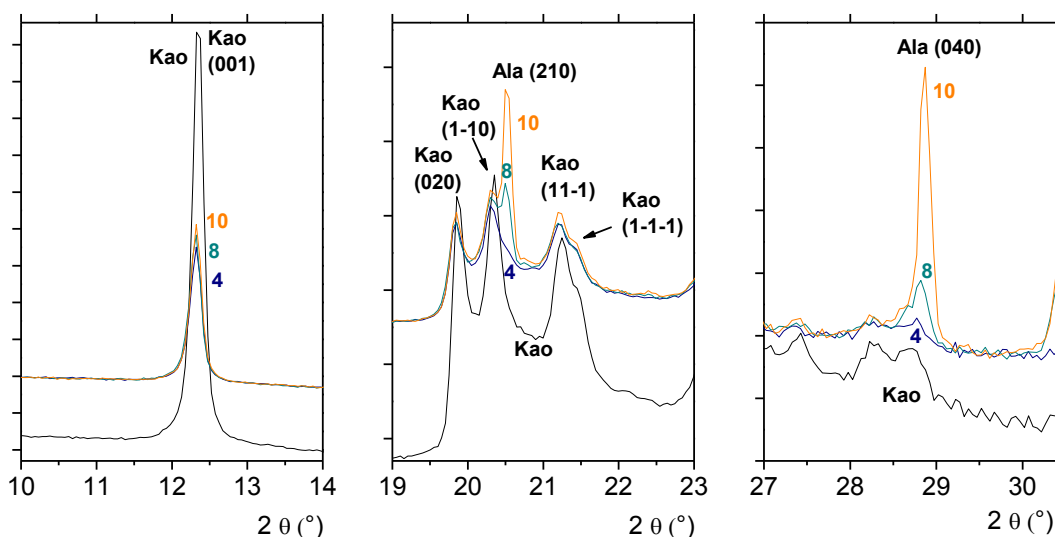
223 *Figure 6: T_{max} of the alanine elimination events, plotted as a function of the amount of*
224 *alanine retained by the Ala/Kao samples. “Peak 1” refers to the minority event shown*
225 *in the right-hand part of Fig.5, “peak 2” to the main (sublimation) event.*

226

227 This, and the general shape of the DTG events with their slow onsets and sharp endings,
228 suggests a zero-order desorption mechanism, probably from small precipitated alanine
229 particles. However, for the samples with the lowest Ala loadings (sample 2, and
230 shoulder in sample 3, see inset of Figure 5), an additional small peak is apparent at a
231 T_{max} of 218 °C. If present in higher-loading samples, it would be obscured by the much
232 more intense sublimation event. We think that it could correspond to the desorption of a
233 minor amount of alanine molecules (at most 0.3% by weight) interacting with specific
234 kaolinite surface sites (such as silanols or aluminols on the edges).

235 XRD confirms the fact that most of the alanine in the solid samples is not interacting
236 with kaolinite. When the alanine loading is increased, the peaks characteristic of bulk
237 alanine start to appear in superposition to those of kaolinite that remain present. Figure
238 7 shows this trend for the two most intense peaks of L-Ala (indexed according to (Shkir
239 et al., 2017)).

240



241 *Figure 7: XRD powder diffractograms of raw kaolinite, and of three Ala/Kao samples*
 242 *with increasing Ala contents.*

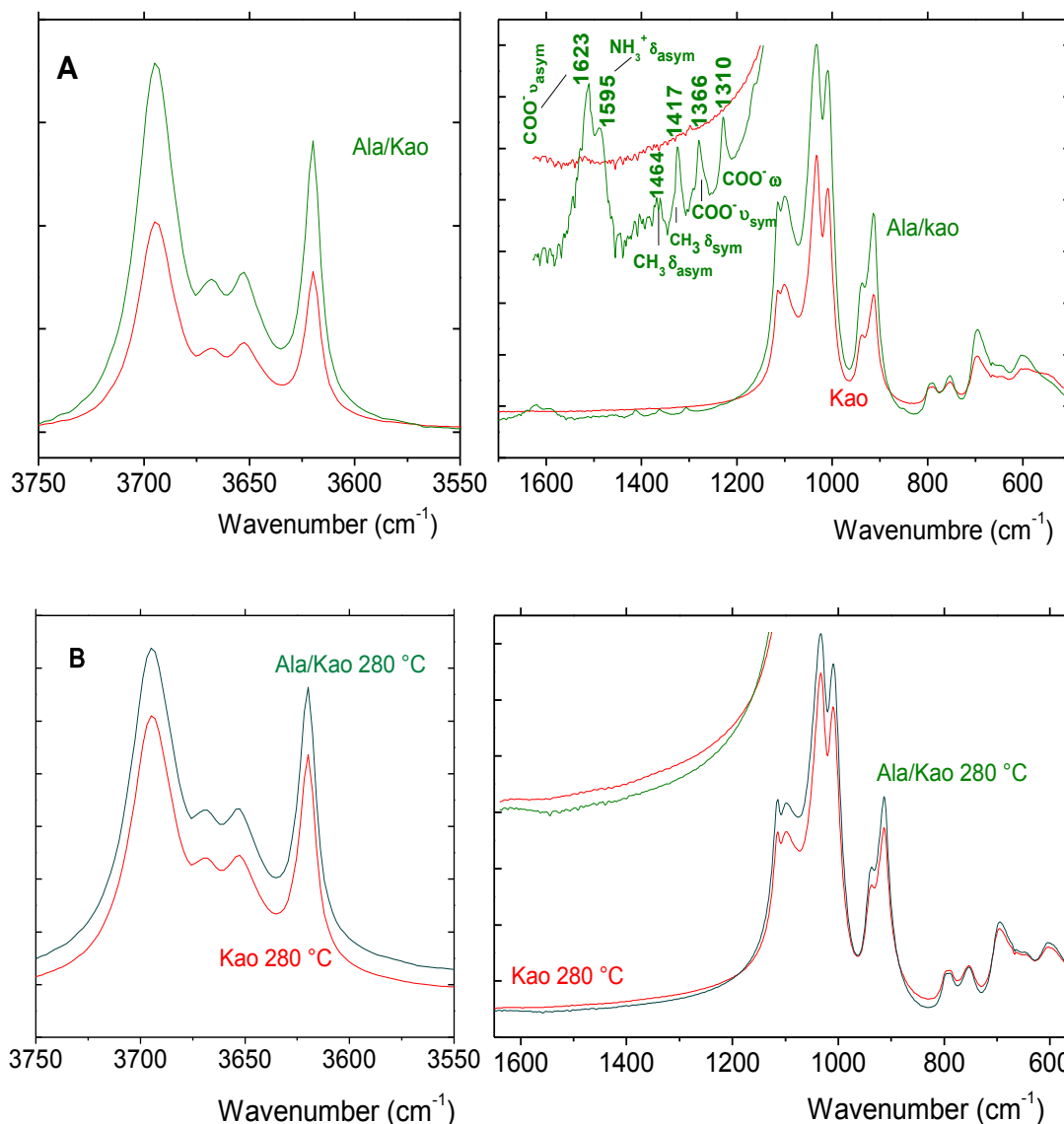
243

244 Peaks indicative of bulk alanine crystallites are discernible when the sample contains at
 245 least 2% Ala. At lower loadings, alanine may be adsorbed on the kaolinite surface,
 246 and/or form crystallites too small and/or in too small quantities to be evidenced by
 247 XRD.

248 Another, negative result must be underlined: the d_{001} of kaolinite is not shifted from its
 249 position in raw kaolinite (7.2 Å), ruling out the possibility of significant alanine
 250 intercalation between the kaolinite layers.

251 The FTIR spectra of the samples are shown in Figure 8. Kaolinite exhibits well-known
 252 signatures in the 550-1200 cm^{-1} (lattice vibrations) and the 3600-3750 cm^{-1} (OH
 253 stretching) regions (Castellano et al., 2010). Figure 8A compares the spectrum of an
 254 Ala/Kao sample with that of raw kaolinite. The former presents a set of sharp, but low-
 255 intensity additional bands in the “fingerprint” region that can all be assigned to the
 256 vibrations of crystalline α -L-Alanine (Rosado et al., 1997) (see inset in right part of the

257 figure). Weak C-H stretching bands are also apparent in the 2850-3000 cm^{-1} region (not
 258 shown). Band positions are listed in Table 4 and compared with those for bulk alanine.
 259 Almost all the expected absorptions are present, with little or no shift from the bulk
 260 positions. This confirms that alanine molecules are intact after deposition, and only
 261 weakly interacting with the surface (no covalent bonds).



262

263

264 *Figure 8: middle IR spectrum of Ala/Kao sample compared with that of raw Kaolinite.*

265

(A) before and (B) after heat treatment at 280 °C.

266

Table 4: Band positions (cm^{-1}) for bulk alanine and Ala/Kao; n.o. = not observed.

Assignment	Position in Ala	Ala/Kao
CH δ	1235	n.o.
NH ₃ ⁺ δ_{sym}	1307	1310
COO ⁻ ν_{sym}	1366	1366
CH ₃ δ_{sym}	1408	1417
CH ₃ δ_{asym}	1458	1464
NH ₃ ⁺ δ_{asym}	1523	n.o.
NH ₃ ⁺ δ_{asym}	1592	1595
COO ⁻ ν_{asym}	1623	1623

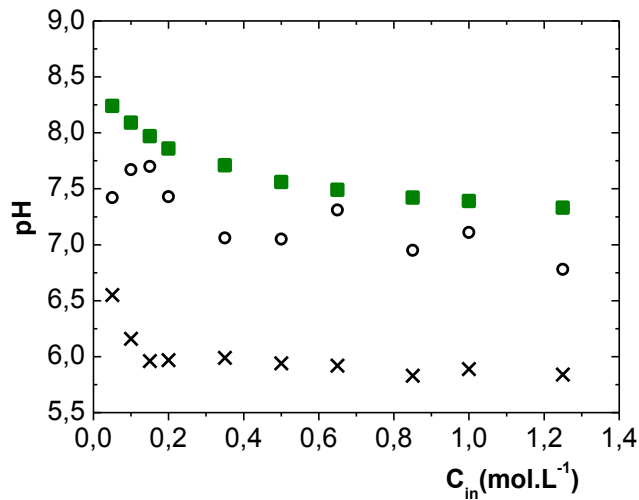
267

268 Figure 8B shows the raw kaolinite and Ala/Kao after heat treatment. The characteristic
269 bands assigned to the vibrations of crystalline α -L-Alanine disappeared after heating up
270 to 280 °C (Completion of thermal event 1). In fact, no bands attributable to adsorbed
271 organic molecules are observable (see magnified fingerprint region in right part of
272 Figure 8 B) and the spectrum is superposable to that of raw kaolinite, confirming the
273 conclusion from TG that all organic matter is desorbed from the solid in the low-
274 temperature event.

275

276 3.2 Alanine on hectorite

277 Upon contact with hectorite, alanine solutions are significantly modified. The pH
278 immediately increases upon contact and a further slow increase is observed upon
279 **equilibrium** (Figure 9), to reach values between 7.3 and 8.3 from the initial 6.2. The
280 strongest increases are observed for the lowest alanine concentrations.



281

282 *Figure 9: pH evolution upon contact of Ala solutions with hectorite, as a function of the*
 283 *initial [Ala] concentration. Crosses, before contact; empty circles, immediately after*
 284 *contact; full squares, after equilibrium.*

285

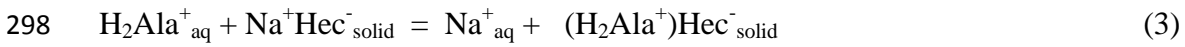
286 This strong variation corresponds to an increase in the base/acid ratio of the
 287 alanine/alaninate couple. These two species can be denoted as HAla^{\pm} and Ala^{-} , the first
 288 symbol underlining the fact that alanine is present as a zwitterion. According to the
 289 well-known Henderson-Hasselbach equation (Eq. 1), one has:

290
$$\text{pH} = \text{pKa} + \log\left(\frac{[\text{Ala}^{-}]}{[\text{HAla}^{\pm}]}\right), \text{ with pKa being the pKa}_2 \text{ of alanine (9.7).} \quad (1)$$

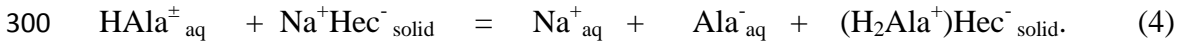
291 Hectorite, in contrast to kaolinite, is a cation exchanger. The original compensating
 292 cations may be substituted by cations present in solution such as the alaninium ions,
 293 H_2Ala^{+} . While they are a very minority species in the solutions we used, the alanine
 294 zwitterion disproportionation reaction, according to equation (2):



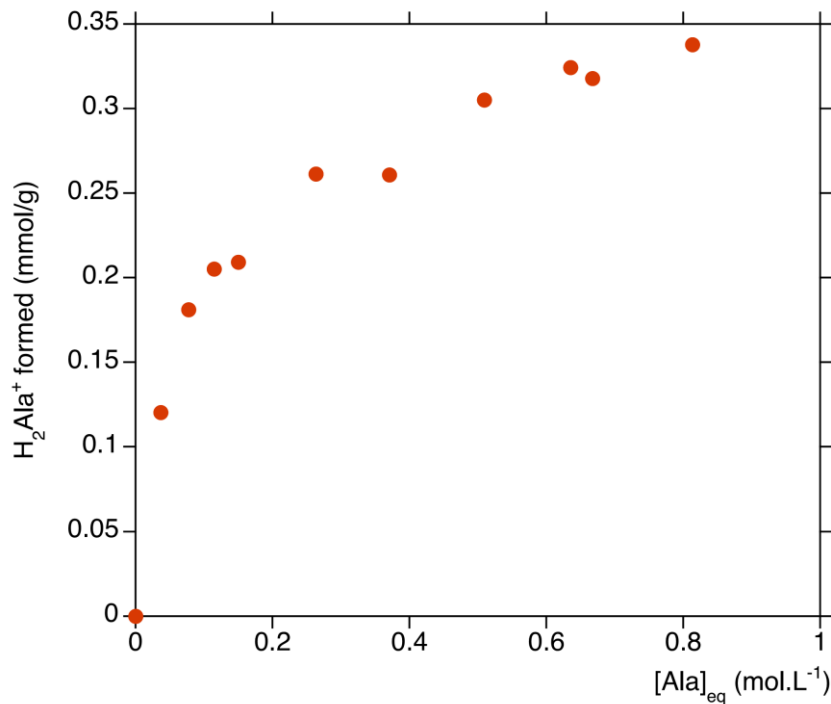
296 would be displaced to the right if the clay (noted as Hec^-) had a strong affinity for
 297 alaninium cations, because it would be coupled to the cation exchange reaction, Eq. (3):



299 so that the global reaction would be the Eq. (4):



301 Thus, in principle, the amount of Ala^- in solution would be equal to the amount of
 302 H_2Ala^+ ion-exchanged. The H_2Ala^+ values estimated from this calculation are plotted as
 303 a function of the equilibrium alanine concentration in Figure 10. The shape of the curve
 304 is indeed reminiscent of those observed for ion exchange in binary systems, but the
 305 maximum amounts remain a factor of three inferior to the CEC.



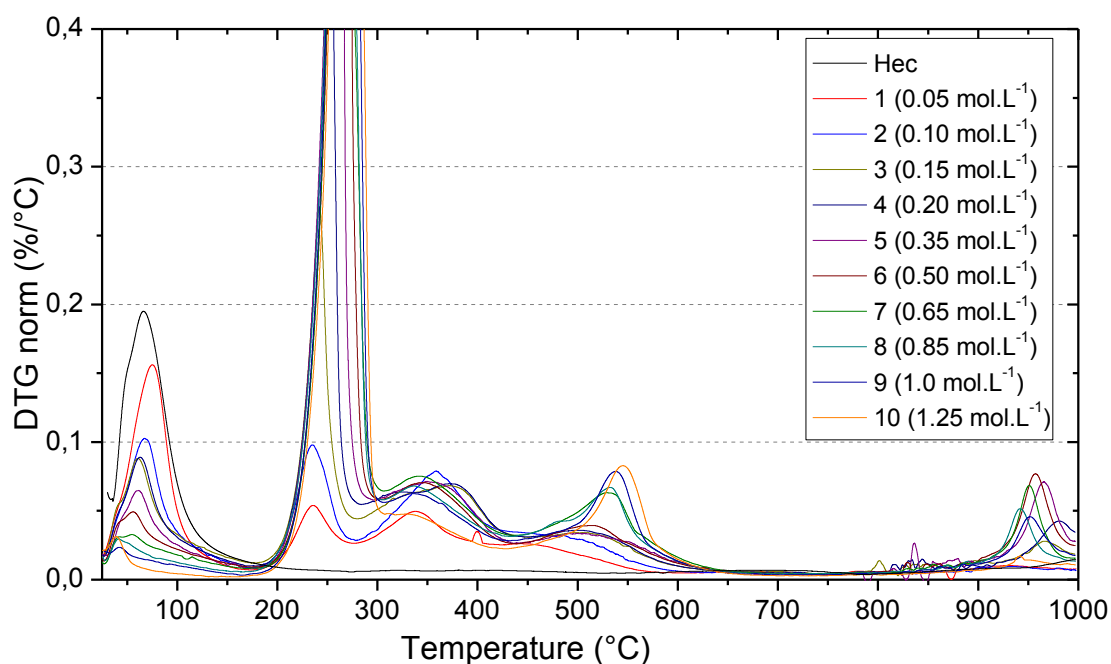
306

307 *Figure 10: Amount of alaninium cations formed (from Henderson-Hasselbach equation)*

308 *as a function of equilibrium alanine concentration in solution*

309 In TG (Figure 11), raw hectorite mostly shows the endothermic elimination of
310 physisorbed water, including water in the interlayers, peaking at 65 °C, and possibly the
311 beginning of a degradation of the hectorite structure, not yet complete at 1000 °C.

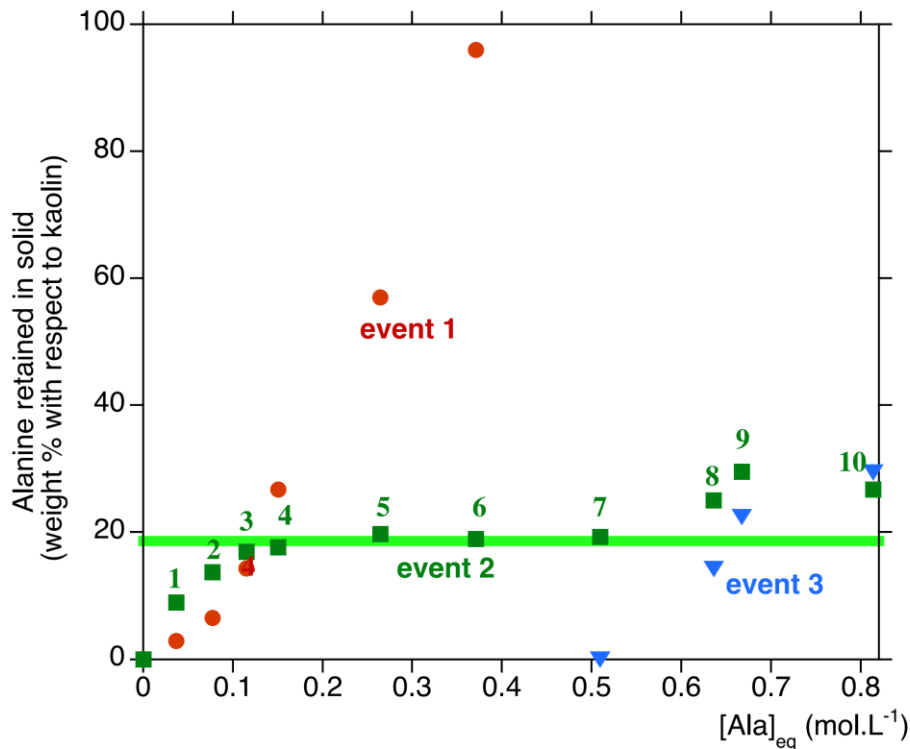
312



313

314 *Figure 11: DTG traces of raw Hectorite, and Ala/Hec samples containing increasing*
315 *amounts of alanine (1 to 10).*

316 Ala/Hec samples show intense peaks in the region of 200-700 °C, indicative of the
317 elimination of a large amount of organic molecules. More specifically, three regions can
318 be identified. The first endothermic event between 200 and 300 °C is present for all
319 samples but strongly increases with the [Ala] concentration in solution. The second
320 event between 300 and 600 °C has a complex shape, is exothermic and partly
321 superimposed on the third event. The latter peaks at 530-545 °C, is strongly exothermic
322 and only appears for the highest loading samples. A quantification of these events is
323 shown in Figure 12.



324

325 *Figure 12: Quantification of the 3 TG events for solid Ala/Hec samples, as a function of*
 326 *the final concentration in solution (increasing concentrations from 1 to 10; event 1 is*
 327 *off scale for samples 7 to 10)*

328

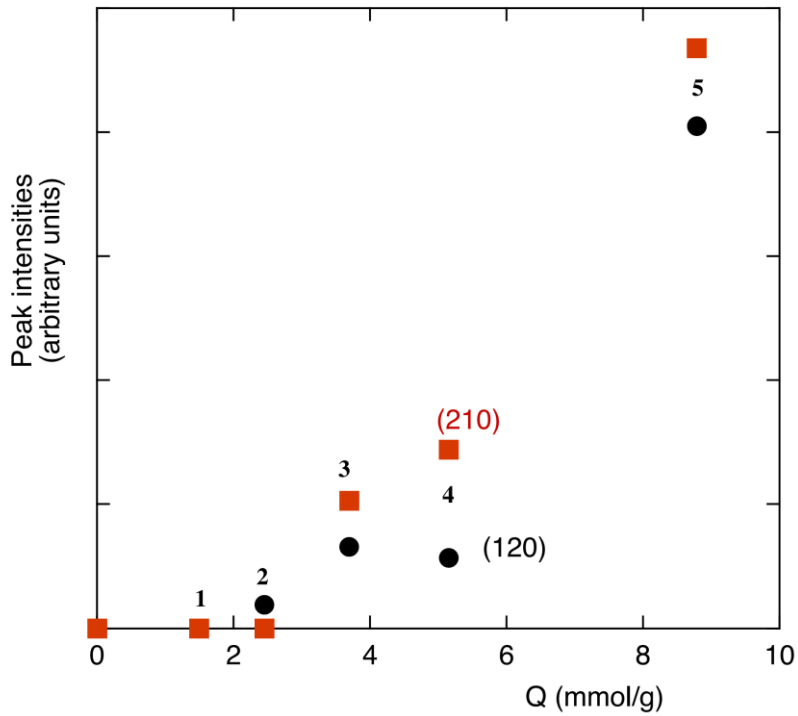
329 For initial Ala concentrations in excess of 0.35 M, the amount of alanine retained in
 330 solid samples is more than 100% of the initial hectorite weight. It seems reasonable to
 331 exclude these samples (7 to 10) from further discussion, at least in the context of
 332 prebiotic chemistry where such situations would be highly unrealistic.

333 Event 1 is very similar to the one we attributed to bulk-like alanine sublimation in
 334 Ala/Kao systems, except that much larger amounts of alanine are retained. The
 335 dependency of the amount corresponding to event 1 on alanine concentration is not
 336 linear however: the retention of bulk-like alanine must involve a phenomenon more
 337 complicated than simple physical retention.

338 The amount corresponding to event 2 follows a different trend, with a possibly
339 Langmuirian shape, reaching a plateau for an amount of alanine of 19% with respect to
340 hectorite, or 2.1 mmol Ala per gram hectorite – to be compared with the CEC, which is
341 1 mmol.g⁻¹. The event is exothermic, meaning that the corresponding alanine molecules
342 do not desorb upon thermal activation – rather, they are eliminated by (possibly
343 catalytic) combustion by oxygen from the air flow.

344 XRD (Figure 13) confirms that alanine crystallites are present starting at least from
345 sample 2, that would contain 6.5% of “bulk-like” alanine according to TG. They are not
346 discernible in sample 1 (2.9% bulk-like alanine). The intensity of alanine peaks
347 increases with the same trend as that of event 1 in TG.

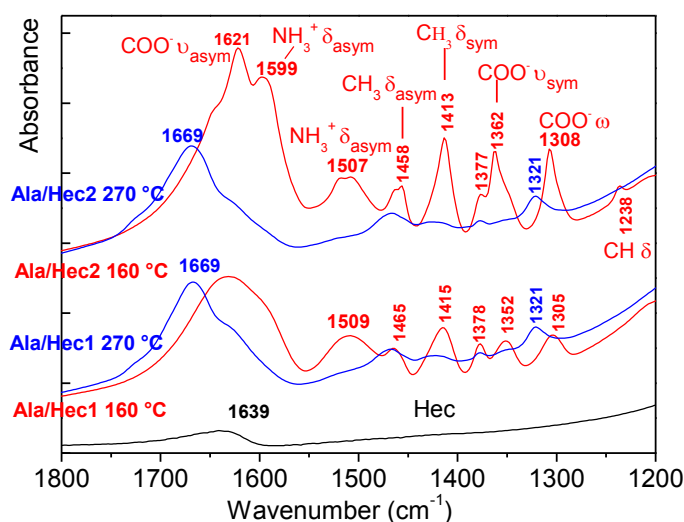
348 The peaks/bands of hectorite remain visible in Ala/Hec although scaled down due to the
349 large amounts of alanine in the samples. This includes the d₀₀₁, which is observed at
350 13.0 Å in raw hectorite, and at 13.8 to 14.05 Å in the alanine-containing samples. It is
351 hard to tell if this indicates intercalation of the organic molecules, since shifts of this
352 order could well simply be due to different hydration states.



353

354 *Figure 13: XRD peak intensities of Ala/Hec samples containing increasing alanine*
 355 *amounts.*

356 For the IR investigations, we concentrated on samples with low alanine loadings, so that
 357 the information on adsorbed alanine species would not be drowned out by the bulk-like
 358 one. Figure 14 presents the IR spectra of the two samples with the lowest alanine
 359 contents. In the fingerprint region, hectorite only has a small band at 1639 cm^{-1} mainly
 360 due to the δ_{HOH} of residual H_2O .



361

362 *Figure 14: middle IR spectrum of Ala/Hec samples 1 and 2 with band assignments*

363

364 The samples contacted with alanine and heated to 160 °C (a temperature where
 365 dehydration is complete but the alanine-associated events have not started yet) show a
 366 series of new bands that can all be assigned to alanine, more especially its zwitterionic
 367 form, as was already the case for Ala/Kao. Most of them (Table 5) are shifted by at
 368 most a few cm^{-1} as compared to bulk alanine. However, the $\text{NH}_3^+ \delta_{\text{asym}}$ is red-shifted by
 369 12-15 cm^{-1} (main band in sample 1, coexists with unshifted in sample 2), and the COO^-
 370 ν_{sym} region appears to show two components: one close to the bulk alanine position, and
 371 a doublet that might result from a splitting of this vibration because of an interaction of
 372 the carboxylate. Thus, at low loadings, a modified form of the zwitterion seems to be
 373 present. The modification would concern both the COO^- and the NH_3^+ moieties; the
 374 accompanying band shifts are larger than those observed for H-bonds, but smaller than
 375 for covalent bonding.

376

377 Table 5: Wavenumbers (cm^{-1}) of vibrational bands of bulk alanine and Ala/Hec. n.o. not
 378 observed.

Assignment	Position in Ala (Rosado et al., 1997; Caroline, et al., 2009; Mohsin, et al. 2018)	Ala/HecS
CH δ	1235	1238
NH ₃ ⁺ δ_{sym}	1307	1305-1308
COO ⁻ ν_{sym}	1366	1377-1378 and 1352 1362 (sample 2 only)
CH ₃ δ_{sym}	1408	1413-1415
CH ₃ δ_{asym}	1458	1458-1465
NH ₃ ⁺ δ_{asym}	1523	1507-1509 1518 (sample 2 only)
NH ₃ ⁺ δ_{asym}	1592	1599
COO ⁻ ν_{asym}	1623	1621

379

380 The spectra are also interesting for what they do not show: COO⁻ and NH₃⁺ are present,
 381 but not the protonated form COOH, which would be evidenced by a C=O stretching at
 382 1730-1750 cm^{-1} . This means that the cationic form (alaninium ion) is either absent or
 383 present in small amounts.

384 After heating up to 270 °C (completion of thermal event 1), strong changes are
 385 observed. The bands attributable to COO⁻ and NH₃⁺ decrease strongly (although they
 386 may not completely disappear), while the CH₃ bands are not affected, and new bands
 387 appear at 1321 and 1669 cm^{-1} . By comparison with similar systems on silica (Sakhno et
 388 al., 2019), the latter is probably an amide I band, the amide groups being formed by
 389 condensation of the ammonium and carboxylates of the original amino acids. Note that
 390 the amide II band expected in the 1500-1600 cm^{-1} region appears to be absent, an
 391 occurrence that has been correlated with the formation of the cyclic dimer
 392 (diketopiperazine).

393

394 **4. Discussion**

395 For the Alanine/kaolinite system, alanine in aqueous solution hardly shows any specific
396 interaction with kaolinite. The solid samples separated from such solutions do contain
397 significant amounts of alanine, but this appears to be due only to physical retention of
398 limited amounts of solution by the solid; when the systems are dried, most of the
399 alanine precipitates in crystals separated from the kaolinite phase, which are apparent
400 upon XRD and IR characterization. Furthermore, the solutions are not significantly
401 modified by contact with kaolinite, except for a small pH drift in the most dilute ones.
402 Careful examination of the DTGs provides evidence for a very small amount of specific
403 adsorption (at most 0.3% by weight). Identification and characterization of species
404 present in such small quantities would require specific spectroscopic techniques, such as
405 solid-state NMR of isotopically marked molecules.

406 Alanine did not form intercalates with kaolinite since the d_{001} was completely
407 unaffected. Such compounds have been reported before (Sato, 1999; Wang et al., 2017),
408 but they used the “guest-exchange” method, i.e. kaolinites pre-swollen with water or
409 ethylene glycol. In a colloidal chemistry study of aspartic acid adsorption on kaolinite,
410 Ikhsan et al (Ikhsan et al., 2004) only found weakly adsorbed molecules, probably by H-
411 bonding, which is compatible with what we observed for alanine.

412 After heat treatment, kaolinite did not retain the alanine adsorbed: it desorbed in a zero-
413 order thermal event before 250 °C. With the techniques we used, there was no evidence
414 of a peptide formation reactivity. Of course, one cannot completely rule out that some
415 peptides were formed and immediately desorbed, but in the present state of
416 investigations this would be a completely ad hoc hypothesis. This lack of peptide bond
417 formation on kaolinite does not stand in contradiction with previously published data.

418 As shown in Table 1, peptide formation on kaolinite was either very minor and/or
419 observed in very different conditions from ours. The most comparable study is probably
420 that of (Dalai et al., 2017), and it showed almost total desorption at 250 °C, in
421 conformity with our observations.

422 The study of the Alanine/hectorite system shows a quite distinct picture. First, the
423 adsorption mechanism is obviously different. The shift to basic pH upon contact with
424 hectorite is well explained if there is a specific intercalation of the cationic form: the
425 selective entrapment of the cationic form from the solution shifts the zwitterion
426 disproportionation balance to the right. X-Ray diffractograms are compatible with
427 alanine intercalation. However, the intercalation may not be completely explained by
428 ion exchange. The amount of ion-exchanged alanine deduced from pH measurements is
429 at most 0.35 mmol.g^{-1} , or one third of the CEC, while the total amount of strongly
430 retained alanine deduced from TG is 2 mmol.g^{-1} , i.e., 6 times higher. Furthermore, IR
431 spectroscopy does not show a clear evidence of the alaninium ion, the species that
432 would be intercalated in an ion-exchange mechanism. Instead, it shows that the
433 predominant alanine species is a zwitterion, whose ammonium and carboxylate moieties
434 are however significantly modified by adsorption. The observed modifications in the
435 carboxylate region may be due to a coordination to remaining Na^+ ions in the interlayer;
436 the ammonium groups, being positively charged, could not take part in the coordinative
437 binding to Na^+ , but they could interact with the negatively charged basal surfaces of
438 hectorite through H-bonding. Thus, the adsorption of alanine on/in hectorite would
439 involve two parallel mechanisms: the cation exchange of protonated alaninium cations
440 (minority), and the coordinative binding of unprotonated alanine zwitterions to
441 remaining compensating cations (majority).

442 After thermal treatment at 270 °C (but not at 160 °C), the Ala/hectorite samples present
443 new FTIR signals indicating the formation of peptide bonds, i.e., amide I bands. The
444 absence of amide II signals can be due to the majority formation of the cyclic dimer of
445 alanine (cyclo-(Ala-Ala), aka dimethyl-DKP). Thus, the strongly adsorbed forms of
446 alanine in hectorite do not desorb upon heating, as opposed to what happens in
447 Alanine/kaolinite, but finally react together to form the cyclic dimers. This reactivity is
448 similar to what has been observed on silica (Guo and Holland, 2015; Lambert et al.,
449 2013) but it needs higher temperatures: on silica, DKP formation is essentially complete
450 at 160 °C, while it has not yet started on hectorite. This may be an illustration of
451 Sabatier's principle for catalysis efficiency: the most effective catalysts for a reaction
452 are those where the reagents/catalyst interaction has just the "right" energy. If the
453 interaction is too weak (as in alanine/kaolinite), the reaction is not catalyzed. If it is too
454 strong (as in alanine/hectorite), the reagents are trapped within the catalyst and take
455 higher activation to react; if the interaction is "just right"(Davies, 2007) (as in
456 alanine/silica), the catalysis is optimal and the reaction may thus proceed at low
457 temperatures.

458 **5. Conclusion**

459 Although peptide formation from amino acids adsorbed on mineral surfaces is a well-
460 established phenomenon, examination of the literature shows that in the case of clay
461 minerals, published results are hard to interpret due to the use of very heterogeneous
462 deposition and activation conditions between the various studies. We have compared in
463 the same conditions two clay minerals with different structures and chemical properties,
464 kaolinite and hectorite, and observed divergent behaviors. On kaolinite, a T:O clay
465 mineral with negligible exchange capacity, alanine was not specifically adsorbed from
466 aqueous solutions, only physically retained. Upon drying, it established at most weak H-

467 bonds with the surface, and upon heating it desorbed extensively with no indication of
468 any prior catalytic reaction on the surface. On hectorite, a T:O:T clay mineral, there was
469 evidence for two simultaneous adsorption mechanisms: a minority cation exchange of
470 the protonated alaninium cation, and a quantitatively more important intercalation
471 probably driven by complexation to the remaining interlayer Na⁺ cations. Amino acids
472 retained by these more energetic mechanisms did not desorb upon heating, but
473 converted to peptides (probably the cyclic DKP) at temperatures comprised between
474 160 and 270 °C. Thus, in order to react, the amino acids must be adsorbed with enough
475 strength to avoid thermal desorption; but the adsorption mechanisms available in
476 smectites such as hectorite are probably too energetic, only allowing reaction at
477 temperatures significantly higher than on silica. Reflexion on the catalytic mechanism
478 for amino acids condensation is probably premature, in view of the lack of consensus
479 for the equivalent reaction on silica supports, even though they have been much more
480 studied. At any rate, our results show that one should be wary of over-generalizing
481 results obtained on a particular support. Amino acids/mineral surfaces systems show a
482 rich and diverse chemistry, and each system must be studied at the molecular level in its
483 own right.

484

485 6. REFERENCES

- 486 Aguilar-Ovando, E., Negrón-Mendoza, A., 2015. Stability of alanine in a high radiation
487 field, adsorbed onto solid surfaces. *J. Radioanal. Nucl. Chem.* 304, 213-217.
488 Bernal, J.D., 1949. The physical basis of life. *Proc. Phys. Soc. London (Section A)* 62,
489 537-558.
490 BU, H., Yuan, P., Liu, H., Liu, D., Quin, Z., Zhong, X., Song, H., Li, Y., 2019.
491 Formation of macromolecules with peptide bonds via the thermal evolution of amino
492 acids in the presence of montmorillonite: Insight into prebiotic geochemistry on the
493 early Earth. *Chem. Geol.* 510, 72–83.
494 Bujdák, J., Rode, B.M., 1997. Silica, alumina, and clay-catalyzed alanine peptide bond
495 formation. *J. Mol. Evol.* 45, 457-466.

496 Bujdák, J., Rode, B.M., 1999a. The effect of clay structure on peptide bond formation
497 catalysis. *J. Mol. Catal. A* 144, 129-136.

498 Bujdák, J., Rode, B.M., 1999b. Silica, alumina, and clay catalyzed peptide bond
499 formation: enhanced efficiency of alumina catalyst. *Orig. Life Evol. Biosph.* 29, 451-
500 461.

501 Bujdák, J., Slosiariková, H., Texler, N., Schwendiger, M., Rode, B.M., 1994. On the
502 possible role of montmorillonite in prebiotic peptide formation. *Monatsh. Chem.* 125,
503 1033-1039.

504 Carneiro, C.E.A., Berndt, G., de Souza Junior, I.G., de Souza, C.M.D., Paesano Jr, A.,
505 da Costa, A.C.S., di Mauro, E., de Santana, H., Zaia, C.T.B.V., Zaia, D.A.M., 2011.
506 Adsorption of Adenine, Cytosine, Thymine, and Uracil on Sulfide-Modified
507 Montmorillonite: FT-IR, Mössbauer and EPR Spectroscopy and X-Ray Diffractometry
508 Studies. *Orig. Life Evol. Biosph.* 41, 453-468.

509 Caroline, M. L., Sankar, R., Indirani, R. M., Vasudevan, S., 2009. Growth, optical,
510 thermal and dielectric studies of an amino acid organic nonlinear optical material: L-
511 Alanine. *Mater. Chem. Phys.* 114, 490-494.

512 Castellano, M., Turturro, A., Riani, P., Montanari, T., Finocchio, E., Ramis, G., Busca,
513 G., 2010. Bulk and surface properties of commercial kaolins. *Appl. Clay Sci.*, 446-454.

514 Dalai, P., Pleyer, H.L., Strasdeit, H., Fox, S., 2017. The Influence of Mineral Matrices
515 on the Thermal Behavior of Glycine. *Orig. Life Evol. Biosph.* 47, 427–452.

516 Davies, P., 2007. *The Goldilocks Enigma: Why is the Universe Just Right for Life?*
517 Penguin, London.

518 Duarte-Silva, R., Villa-Garcia, M.A., Rendueles, M., Diaz, M., 2014. Structural,
519 textural and protein adsorption properties of kaolinite and surface modified kaolinite
520 adsorbents. *Appl. Clay Sci.* 90, 73–80.

521 Fontecilla Camps, J.C., 2019. Geochemical Continuity and Catalyst/Cofactor
522 Replacement in the Emergence and Evolution of Life. *Angew. Chem.* 58, 42-48.

523 Georgelin, T., Jaber, M., Fournier, F., Laurent, G., Costa-Torro, F., Maurel, M.-C.,
524 Lambert, J.-F., 2015. Stabilization of ribofuranose by a mineral surface. *Carbohydr.*
525 *Res.* 402, 241-244.

526 Guo, C.C., Holland, G.P., 2015. Alanine Adsorption and Thermal Condensation at the
527 Interface of Fumed Silica Nanoparticles: A Solid-state NMR Investigation. *J. Phys.*
528 *Chem. C* 119, 25663-25672

529 Ikhsan, J., Johnson, B.B., Wells, J.D., Angove, M.J., 2004. Adsorption of aspartic acid
530 on kaolinite. *J. Coll. Interf. Sci.* 273, 1-5.

531 Ito, M., Handa, N., Yanagawa, H., 1990. Synthesis of polypeptides by microwave
532 heating I. Function of polypeptides synthesized during repeated hydration-dehydration
533 cycles. *J. Mol. Evol.* 31, 187-194.

534 Jaber, M., Georgelin, T., Bazzi, H., Costa-Torro, F., Lambert, J.-F.o., Bolbach, G.r.,
535 Clodic, G., 2014. Selectivities in Adsorption and Peptidic Condensation in the (Arginine
536 and Glutamic Acid)/Montmorillonite Clay System. *J. Phys. Chem. C* 118,
537 25447–25455.

538 Jackson, T.A., 1971. Preferential Polymerization and Adsorption of L-Optical Isomers
539 of Amino Acids Relative to D-Optical Isomers on Kaolinite Templates. *Chem. Geol.* 7,
540 295-306.

541 Kalra, S., Pant, C.K., Pathak, H.D., Mehta, M.S., 2000. Adsorption of glycine and
542 alanine on montmorillonite with or without co-ordinated divalent cations. *Ind. J.*
543 *Biochem. Biophys.* 37, 341-346.

544 Kollár, T., Pálinkó, I., Kónya, Z., Kiricsi, I., 2003. Intercalating amino acid guests into
545 montmorillonite host. *J. Mol. Struct.* 651–653, 335–340.

546 Lahav, N., White, D., Chang, S., 1978. Peptide formation in prebiotic era - thermal
547 condensation of glycine in fluctuating clays environments. *Science* 201, 67-69.

548 Lambert, J.-F., 2008. Adsorption and polymerization of amino acids on mineral
549 surfaces: A review. *Orig. Life Evol. Biosph.* 38, 211-242.

550 Lambert, J.-F., Jaber, M., Georgelin, T., Stievano, L., 2013. A comparative study of the
551 catalysis of peptide bond formation by oxide surfaces. *Phys. Chem. Chem. Phys.* 15,
552 13371 - 13380.

553 Lambert, J.-F., Millman, W.S., Fripiat, J.J., 1989. Revisiting kaolinite dehydroxylation:
554 A ²⁹Si and ²⁷Al MAS-NMR study. *J. Am. Chem. Soc.* 111, 3517-3522.

555 Le Son, H., Suwannachot, Y., Bujdák, J., Rode, B.M., 1998. Salt-induced peptide
556 formation from amino acids in the presence of clays and related catalysts. *Inorg. Chem.*
557 *Acta* 272, 89-94.

558 Martra, G., Deiana, C., Sakhno, Y., Barberis, I., Fabbiani, M., Pazzi, M., Vincenti, M.,
559 2014. The Formation and Self-Assembly of Long Prebiotic Oligomers Produced by the
560 Condensation of Unactivated Amino Acids on Oxide Surfaces. *Angew. Chem.* 53, 4671
561 -4674.

562 Meng, M., Xia, L.Y., Guo, L.H., 2007. Adsorption and Thermal Condensation of
563 Glycine on Kaolinite. *Acta Phys. Chim. Sin.* 23, 32-36.

564 Mohsin, G. F., Schmitt, F.-J., Kanzler, C., Epping, J. D., Flemig, S., Hornemann, A.,
565 2018. Structural characterization of melanoidin formed from D-glucose and L- alanine
566 at different temperatures applying FTIR, NMR, EPR, and MALDI- ToF-MS. *Food*
567 *Chem.* 245, 761-767.

568 Paecht-Horowitz, M., 1978. The Influence of Various Cations on the Catalytic
569 Properties of Clays. *J. Mol. Evol.* 11, 101-107.

570 Paecht-Horowitz, M., Berger, J., Katchalsky, A., 1970. Prebiotic Synthesis of
571 Oligopeptides by Heterogeneous Polycondensation of Amino-Acid Adenylates. *J. Mol.*
572 *Evol.* 228, 636-639.

573 Pedreira-Segade, U., Feuillie, C., Pelletier, M., Michot, L.J., Daniel, I., 2016.
574 Adsorption of nucleotides onto ferromagnesian phyllosilicates: Significance for the
575 origin of life. *Geochim. Cosmochim. Acta* 176, 81-95.

576 Ponnampereuma, C., Simoyama, A., Friebele, E., 1982. Clay and the origin of life. *Orig.*
577 *Life* 12, 9-40.

578 Porter, T.L., Eastman, M.P., Bain, E., Begay, S., 2001. Analysis of peptides synthesized
579 in the presence of SAz-1 montmorillonite and Cu² exchanged hectorite. *Biophys.*
580 *Chem.* 91, 115-124.

581 Porter, T.L., Eastman, M.P., Hagerman, M.E., Price, L.B., Shand, R.F., 1998. Site-
582 Specific Prebiotic Oligomerization Reactions of Glycine on the Surface of Hectorite. *J.*
583 *Mol. Evol.* 47, 373-377.

584 Ramos, M.E., Huertas, F.J., 2013. Adsorption of glycine on montmorillonite in aqueous
585 solutions. *Appl. Clay Sci.* 80-81, 10-17.

586 Rosado, M.T.S., Duarte, M.L.R.S., Fausto, R., 1997. Vibrational spectra (FT-IR, Raman
587 and MI-IR) of α and β -alanine. *J. Mol. Struct.* 410-411, 343-348.

588 Sakhno, Y., Battistella, A., Mezzetti, A., Jaber, M., Georgelin, T., Michot, L., Lambert,
589 J.-F., 2019. One step up the ladder of prebiotic complexity: Formation of non- random
590 linear polypeptides from binary systems of amino acids on silica. *Chem. Eur. J.* 25,
591 1275-1285

592 Sato, M., 1999. Preparation of Kaolinite-Amino Acid Intercalates Derived from
593 Hydrated Kaolinite. *Clays Clay Min.* 47, 793-802.

594 Shkir, M., Yahia, I.S., Al-Qahtani, A.M.A., Ganesh, V., AlFaity, S., 2017. Investigation
595 on physical properties of L-alanine: An effect of Methylene blue dye. *J. Mol. Struct.*
596 1113, 43-50.

597 Spence, A., Kelleher, B.P., 2012. FT-IR spectroscopic analysis of kaolinite–microbial
598 interactions. *Vibr. Spectr.* 61, 151–155.

599 Villafane-Barajas, S.A., Bau, J.P.T., Colin-Garcia, M., Negron-Mendoza, A., Heredia-
600 Barbero, A., Pi-Puig, T., Zaia, D.A.M., 2018. Salinity Effects on the Adsorption of
601 Nucleic Acid Compounds on Na-Montmorillonite: a Prebiotic Chemistry Experiment.
602 *Orig. Life Evol. Biosph.* 48, 181-200.

603 Wang, Z.R., Zheng, W., Zhang, Z.Q., Chen, L.K., Zhang, Z.F., Li, Y., Ma, N., Du, P.Y.,
604 2017. Formation of a kaolinite-serine intercalation compound via exchange of the pre-
605 intercalated transition molecules in kaolinite with serine. *Appl. Clay Sci.* 135, 378–385.

606 White, D.H., Kennedy, R.M., Macklin, J., 1984. Acyl silicates and acyl aluminates as
607 activated intermediates in peptide formation on clays. *Orig. Life* 14, 273-278.

608 Yang, D.Y., Peng, S.M., Hartman, M.R., Gupton-Campolongo, T., Rice, E.J., Chang,
609 A.K., Gu, Z., Lu, G.Q.M., Luo, D., 2013. Enhanced transcription and translation in clay
610 hydrogel and implications for early life evolution. *Scient. Rep.* 3, 3165.

611 Zaia, D.A.M., 2012. Adsorption of amino acids and nucleic acid bases onto minerals: a
612 few suggestions for prebiotic chemistry experiments. *Int. J. Astrobiol.* 11, 229-234.

613 Zamaraev, K.I., N.Romannikov, V., Salganik, R.I., Wlassoff, W.A., Khramtsov, V.V.,
614 1997. Modelling of the prebiotic synthesis of oligopeptides: silicate catalysts help to
615 overcome the critical stage. *Orig. Life Evol. Biosph.* 27, 325-337.

616